



Supporting Information

for *Adv. Sci.*, DOI: 10.1002/advs.201500359

Antiperovskite Li_3OCl Superionic Conductor Films for Solid-State Li-Ion Batteries

Xujie Lü, John W. Howard, Aiping Chen, Jinlong Zhu, Shuai Li, Gang Wu, Paul Dowden, Hongwu Xu, Yusheng Zhao,* and Quanxi Jia**

Supporting Information

Anti-Perovskite Li₃OCl Superionic Conductor Films for Solid-State Li-Ion Batteries

Xujie Li,^{} John W. Howard, Aiping Chen, Jinlong Zhu, Shuai Li, Gang Wu, Paul Dowden, Hongwu Xu, Yusheng Zhao,^{*} and Quanxi Jia^{*}*

Experimental details*Target preparation and film deposition:*

To prepare the composite target for pulsed laser deposition of Li₃OCl films, Li₂O (Aldrich, 97% purity) and LiCl powders (Aldrich, 99% purity) with stoichiometric ratios were mixed and ground thoroughly in an Ar-filled glove box. The mixed powders were pressed into a pellet at a pressure of 3000 psi. The pellet was annealed at 350 °C in a controlled environment (Ar protection) for 4 hours. The XRD pattern in Figure 1a clearly indicates that the annealing process for target preparation does not result in obvious chemical reaction between the raw materials.

The Li₃OCl films were deposited on Li-coated silicon and polished stainless steel substrates by PLD (KrF laser, 248 nm, 20 Hz) under vacuum (1×10^{-5} Torr) using the as-prepared composite target. A protective layer of ZnO was deposited on top of the Li₃OCl films without breaking the vacuum (simply by switching the targets) to prevent Li₃OCl from direct exposure to air during XRD and SEM measurements. The multi-layer films of Au/Li₃OCl/Au and Li/Li₃OCl/Li were deposited without breaking the vacuum to study the ionic conductivity, cyclability, and compatibility with lithium metal of the Li₃OCl films. The detailed PLD parameters for the deposition of different materials are shown in Table S1.

Characterizations and electrochemical measurements:

The structure of the films was studied by X-ray diffraction (XRD, Rigaku Ultima III), and the interfacial characteristic between Li₃OCl and Li metal was investigated by scanning electron microscopy (SEM) instrument equipped with an in-situ Focused Ion Beam (FIB)

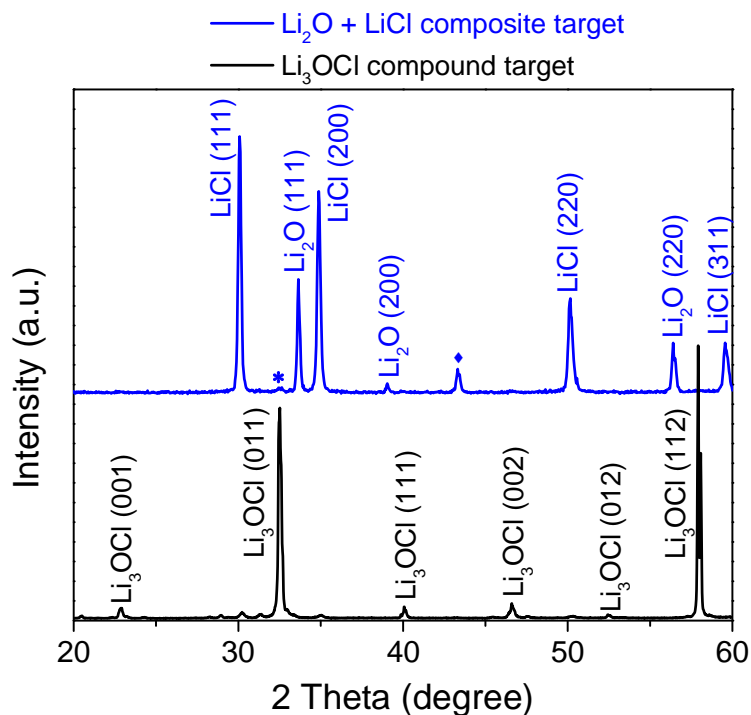
system. Electrochemical measurements were carried out using an air-tight cell. AC electrochemical impedance spectroscopy (EIS) measurements were conducted in the frequency range from 100 Hz to 4 MHz with a voltage amplitude of 10 mV by using an electrochemical system (PARSTAT 2273, Princeton Applied Research). The temperature was controlled from room temperature to 140 °C. The ionic conductivities and the activation energy of the Li_3OCl films were derived from the impedance spectra. The symmetric cell of $\text{Li}/\text{Li}_3\text{OCl}/\text{Li}$ was cycled by applying a constant current of 1.0 mA with periodically changed polarity using a battery test station (Arbin BT-2000) at room temperature. Full solid-state LIBs with a configuration of graphite/ $\text{Li}_3\text{OCl}/\text{LiCoO}_2$ were constructed via a layer-by-layer deposition route, and the cycling tests were carried out between 2.2 and 4.2 V at an applied current of 10 mA g^{-1} at room temperature. The morphologies of graphite anode and LiCoO_2 cathode used in the full batteries are shown in Figure S3.

Table S1. PLD parameters used for deposition of different materials. The KrF laser with wavelength of 248 nm was used.

| Films | Li_3OCl layer | ZnO layer | Au layer | Li layer | LiCoO_2 layer |
|---|---|--|--|--|--|
| $\text{Li}_3\text{OCl}/\text{ZnO}$ | 4.0 J cm^{-2} 30 Hz, 60 min, 175 °C, vacuum | 4.0 J cm^{-2} 30 Hz, 30 min, 175 °C, 50 mTorr Ar | N/A | N/A | N/A |
| $\text{Au}/\text{Li}_3\text{OCl}/\text{Au}$ | 4.0 J cm^{-2} 30 Hz, 60 min, 175 °C, vacuum | N/A | 6.0 J cm^{-2} 20 Hz, 60 min, 175 °C, 50 mTorr Ar | N/A | N/A |
| $\text{Li}/\text{Li}_3\text{OCl}/\text{Li}$ | 4.0 J cm^{-2} 30 Hz, 60 min, 175 °C, vacuum | N/A | N/A | 2.0 J cm^{-2} 30 Hz, 60 min, 175 °C 50 mTorr Ar | N/A |
| $\text{C}/\text{Li}_3\text{OCl}/\text{LiCoO}_2$ | 4.0 J cm^{-2} 30 Hz, 60 min, 175 °C, vacuum | N/A | N/A | N/A | 5.0 J cm^{-2} 10 Hz, 30 min, 200 °C, 75 mTorr O_2 |
| $\text{Li}/\text{Li}_3\text{OCl}/\text{ZnO}$ | 4.0 J cm^{-2} 30 Hz, 60 min, 175 °C, vacuum | 4.0 J cm^{-2} 30 Hz, 30 min, 175 °C, 50 mTorr Ar | N/A | 2.0 J cm^{-2} 30 Hz, 60 min, 175 °C 50 mTorr Ar | N/A |

Table S2. Summary of properties and synthetic methods for various solid-state electrolytes.

| Electrolytes | σ at RT (S cm ⁻¹) | E_a (eV) | Working window | Stability with Li | Synthesis methods |
|--|---|---------------|-------------------|----------------------|---------------------------------|
| Li ₃ OCl in this work | 2×10^{-4} | 0.35 | > 5 V | Stable | Pulsed laser deposition |
| Li ₃ OCl in reference ^[1] | 9×10^{-6} | 0.36 | > 5 V | Stable | Pulsed laser deposition |
| LiPON ^[2-3] | 10^{-6} | 0.7 | 1.0–5.0 V | Stable | Sputtering |
| Single-crystal Li ₃ N ^[4] | 10^{-3} | 0.25 | N/A | Stable | Czochralski technique |
| Li ₁₄ Zn(GeO ₄) ₄ ^[5] | 10^{-6} | 0.42 | N/A | Unstable | Solid state reaction |
| Li ₇ La ₃ Zr ₂ O ₁₂ ^[6] | 10^{-4} | 0.36 | >3V | Stable | Solid state reaction |
| γ -Li ₃ PS ₄ ^[7] | 10^{-7} | 0.49 | N/A | Unstable | Solid state reaction |
| β -Li ₃ PS ₄ (nano) ^[8] | 10^{-4} | 0.35 | > 5 V | Unstable | THF-assisted solution method |
| Li ₄ SnS ₄ ^[9] | 10^{-5} | 0.4 | > 5 V | Unstable | Solid state reaction |

Figures**Figure S1.** XRD patterns of Li₂O + LiCl composite target and fully reacted Li₃OCl compound target. The symbol of ♦ indicates the peak from Cu holder.

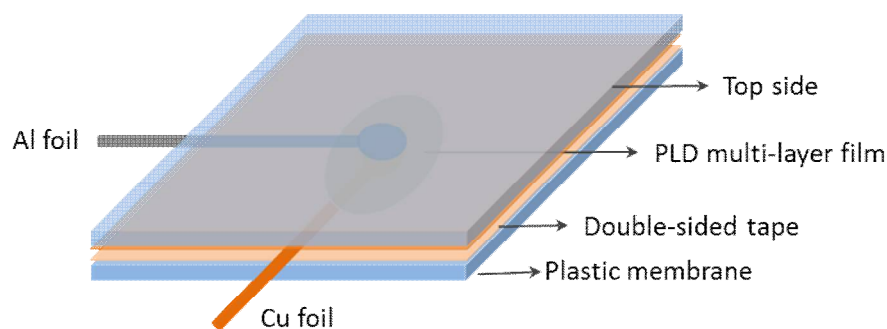


Figure S2. Schematic structure of the membrane-type solid-state Li-ion battery.

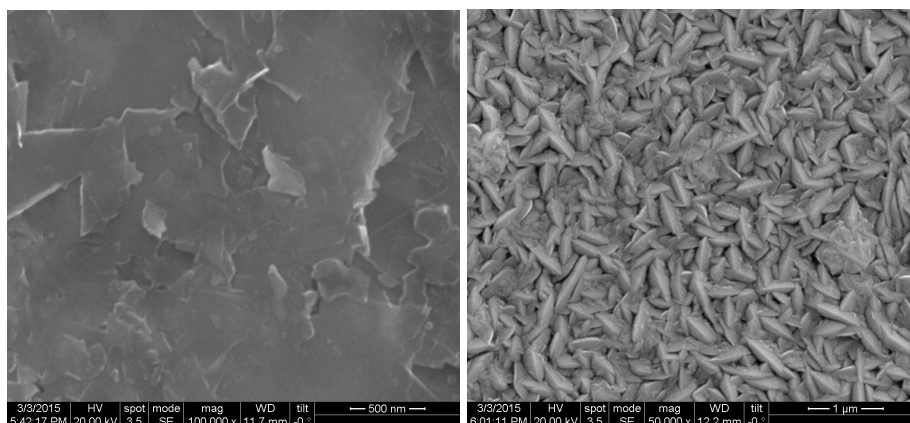


Figure S3. SEM images of graphite anode (left) and LiCoO₂ cathode (right) used in the full thin-film LIBs.

References

- [1] X. Lü, G. Wu, J. W. Howard, A. Chen, Y. Zhao, L. L. Daemen, Q. Jia, *Chem. Commun.* **2014**, *50*, 11520-11522.
- [2] H. Y. Park, S. C. Nam, Y. C. Lim, K. G. Choi, K. C. Lee, G. B. Park, S.-R. Lee, H. P. Kim, S. B. Cho, *J. Electroceram.* **2006**, *17*, 1023-1030.
- [3] F. Muñoz, A. Durán, L. Pascual, L. Montagne, B. Revel, A. C. M. Rodrigues, *Solid State Ionics* **2008**, *179*, 574-579.
- [4] U. v. Alpen, A. Rabenau, G. H. Talat, *Appl. Phys.Lett.* **1977**, *30*, 621-623.
- [5] U. v. Alpen, M. F. Bell, W. Wichelhaus, K. Y. Cheung, G. J. Dudley, *Electrochim. Acta* **1978**, *23*, 1395-1397.

- [6] A. Kaeriyama, H. Munakata, K. Kajihara, K. Kanamura, Y. Sato, T. Yoshida, *ECS Transactions* **2009**, *16*, 175-180.
- [7] M. Tachez, J.-P. Malugani, R. Mercier, G. Robert, *Solid State Ionics* **1984**, *14*, 181-185.
- [8] Z. Liu, W. Fu, E. A. Payzant, X. Yu, Z. Wu, N. J. Dudney, J. Kiggans, K. Hong, A. J. Rondinone, C. Liang, *J. Am. Chem. Soc.* **2013**, *135*, 975-978.
- [9] G. Sahu, Z. Lin, J. Li, Z. Liu, N. Dudney, C. Liang, *Energy Environ. Sci.* **2014**, *7*, 1053-1058.